Romanian Reports in Physics **70**, 203 (2018)

CROSS SECTIONS FOR ELECTRON CAPTURE IN $\mathrm{Li}^{3+} + \mathrm{H}(1s)$ COLLISIONS IN DEBYE PLASMAS

M. C. RAPORTARU[1], L. BARANDOVSKI[2], N. STOJANOV[2], D. JAKIMOVSKI[2,*]

[1]Department of Computational Physics and Information Technologies,
Horia Hulubei National Institute for Physics and Nuclear Engineering,
Reactorului 30, Magurele, Ilfov, Romania
[2]Institute of Physics, Faculty of Natural Sciences and Mathematics,
Gazi baba bb, Skopje, Macedonia
[*]Corresponding author, Email: dragan.jakimovski@gmail.com

Received August 7, 2017

Abstract. Electron capture in collisions of Li^{3+} ion with hydrogen atom in ground state in Debye plasma is studied by employing the two-center atomic orbital close-coupling method. The plasma screened interaction of the electron with the two centers is represented by the Debye-Hückel potential, appropriate for a wide class of laboratory and astrophysical plasmas (Debye plasmas). The sensitivity of $nl-$ selective capture sections to interaction screening, as well as the electron capture enhancement in Debye plasmas in the low-energy region are confirmed. The bell-shaped local maxima of the dependence of the $2l$ partial sections in a region of screening length D, for lower energy, is attributed to the proximity (and intersection) of the energies of the initial and final levels in that region.

Key words: electron capture, collisions, plasma.

1. INTRODUCTION

Collisions between charged and neutral particles, at all velocities, are effective in transitions of any mixture of neutral gases to plasma and have significant role in establishing its parameters - density, temperature, electrical conductivity, and radiative dissipation of energy, to name a few. Excitation and charge exchange, as well as ionization and capture of free electrons, are key physical mechanisms for changing their values. The plethora of theoretical and experimental work has been devoted to research and improving the knowledge in this field in a span of several decades (see, *e.g.* [1–3] and references therein).

For thermonuclear plasmas it is important to have corresponding quantitative information for some specific ions, which are considered as impurities in fusion context, as these ions may decrease its temperature. They usually originate from atoms with nuclear charges $Z \leq 9$ and enter the plasma from the compartment walls of the functioning tokamaks, due to desorption, but may be due to deliberate injection too, for plasma cooling or for diagnostic purposes. As they enter the regions with

higher temperature they progressively become more ionized, up to, and including fully stripped, bare ions, versions of these impurities.

Beryllium, tungsten, and lithium are among the most frequently used, or explored to be used, as materials for various designed parts of operating reactors or of those planned for future fusion experiments, including ITER (the International Thermonuclear Experimental Reactor) [4]. Lithium beams and lithium pellets are used for diagnostics of tokamak edge plasma parameters for some time now [5] and the innovative concept of using liquid lithium as coating for the divertor plates brings these chemical species once again into the focus of the plasma community (see [6] and the references therein).

In the present work we will study the electron capture process

$$\mathrm{Li}^{3+} + \mathrm{H}(1s) \rightarrow \mathrm{Li}^{2+}(nl) + \mathrm{H}^{+} \tag{1}$$

when the effective interaction between the electron and the lithium ion may be described by the Debye-Hückel potential

$$V(r) = -\frac{Ze^2}{r} e^{-r/D}, \tag{2}$$

where e is the unit charge, $Z = 3$ for fully stripped lithium ions and D is the Debye screening length, related to the plasma electron temperature (T_e) and the plasma density (n_e) by the relation $\mathrm{D} = (k_{\mathrm{B}} T_e/(4\pi e^2 n_e))^{1/2}$, k_{B} being the Boltzmann constant. This potential is appropriate to use when these two conditions are met : $\Gamma \leq 1$ for $\Gamma = e^2/(a k_{\mathrm{B}} T_e)$ (Coulomb coupling parameter) and $\gamma \ll 1$ for $\gamma = e^2/(D k_{\mathrm{B}} T_e)$ (plasma non-ideality parameter), where $a = [3/(4\pi n_e)]^{1/3}$ is the average inter-particle distance.

In our study of the electron capture process (1) we will employ the two-center atomic orbital (TC-AOCC) method with adequate expansion basis to include the dominantly populated shells of the Li^{2+}. In the next Section we outline the method itself and the computational details, followed by the results and the conclusion Sections.

Atomic units will be used in the following, unless explicitly stated otherwise.

2. METHOD AND COMPUTATIONAL DETAILS

The calculations of the cross sections for electron capture have been performed within the framework of the semiclassical two-center atomic orbital method. The details of the method are discussed extensively elsewhere [3, 7] so here we will present only its main points. The total electron wave function for one-electron two-center system is expanded in terms of electronic states centered on the proton and on the Li^{3+}. These states are traveling atomic orbitals, determined by the variational method

with even-tempered trial functions [8, 9]

$$\chi_{klm}(\mathbf{r};\mathrm{D}) = N_l(\xi_k(\mathrm{D}))\, r^l e^{-\xi_k(\mathrm{D})r} Y_{lm}(\hat{\mathbf{r}}) \tag{3}$$

$$\xi_k(\mathrm{D}) = \alpha\beta^k,\ \ k = 1, 2, \cdots, N,$$

where $N_l(\xi_k)$ is a normalization constant, $Y_{lm}(\hat{\mathbf{r}})$ are the spherical harmonic functions and α and β are two variational parameters determined by minimization of the energy for each value of the screening length D. The atomic states $\phi_{nlm}(\mathbf{r};\mathrm{D})$ are then obtained as linear combinations

$$\phi_{nlm}(\mathbf{r};\mathrm{D}) = \sum_k c_{nk}\chi_{klm}(\mathbf{r};\mathrm{D}) \tag{4}$$

with the coefficients c_{nk} being determined by diagonalizing the corresponding single-centre Hamiltonian. This diagonalization gives the energies $E_{nl}(\mathrm{D})$ of the electron states.

The relative motion of the two centers of this collisional systems is approximated to be classical, along a straight−line $\mathbf{R}(t) = \mathbf{b} + \mathbf{v}t$ (where $\mathbf{b}$ is the impact parameter and $\mathbf{v}$ is the collision velocity). By expanding the total electron wave function Ψ in terms of atomic orbitals (with plane wave electron translational factors) centered on the target (T) and projectile (P) and traveling along this straight line [7]

$$\Psi(\mathbf{r},t;\mathrm{D}) = \sum_i a_i(t)\,\phi_i^T(\mathbf{r},t;\mathrm{D}) + \sum_j b_j(t)\,\phi_j^P(\mathbf{r},t;\mathrm{D}) \tag{5}$$

and inserting it in the time-dependent Schrödinger equation

$$\left(-\frac{1}{2}\nabla_r^2 + V_T(r_T) + V_P(r_P) - i\frac{\partial}{\partial t}\right)\Psi = 0, \tag{6}$$

where $V_{T,P}(r_{T,P})$ are the electron interactions with the target proton and the projectile, respectively, one obtains the coupled equations for the amplitudes $a_i(t)$ and $b_j(t)$

$$i(\dot{\mathbf{A}} + \mathbf{S}\dot{\mathbf{B}}) = \mathbf{H}\mathbf{A} + \mathbf{K}\mathbf{B}, \tag{7a}$$

$$i(\dot{\mathbf{B}} + \mathbf{S}^\dagger\dot{\mathbf{A}}) = \bar{\mathbf{K}}\mathbf{A} + \bar{\mathbf{H}}\mathbf{B}, \tag{7b}$$

where $\mathbf{A}$ and $\mathbf{B}$ are the vectors of the amplitudes $a_i(t)$ and $b_j(t)$, respectively. $\mathbf{S}$ is the overlap matrix ($\mathbf{S}^\dagger$ is its transposed form), $\mathbf{H}$ and $\bar{\mathbf{H}}$ are direct coupling matrices involving the states on the projectile and target, respectively, and $\mathbf{K}$ and $\bar{\mathbf{K}}$ are the $i-j$ and $j-i$ electron exchange matrices.

The solutions of the system of equations under the initial conditions $a_i(-\infty) = \delta_{1i}$, $b_j(-\infty) = 0$, yield for the $1 \to i$ excitation and $1 \to j$ charge exchange cross

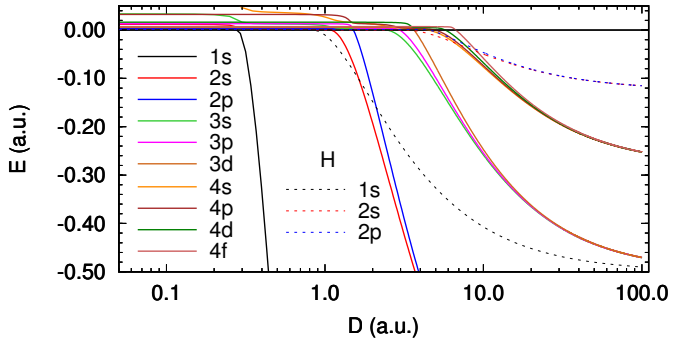

Fig. 1 – (Color online) Energies of $n \leq 4$ states of Li^{2+} ion for an interval of screenings D up to 100 a.u. (full lines) with corresponding $1s$ and $2l$ levels of H atom (broken lines).

sections the following expressions

$$\sigma_{ex,i} = 2\pi \int_0^\infty |a_i(+\infty)|^2 b db, \tag{8a}$$

$$\sigma_{cx,j} = 2\pi \int_0^\infty |b_j(+\infty)|^2 b db, \tag{8b}$$

where b is the impact parameter.

The validity of this semiclassical TC-AOCC method in an ion-atom collision with pure Coulomb interaction between the two heavy centers and the electron hangs on the applicability of the classical description for the relative nuclear motion and the size of the expansion, small enough to be computationally feasible but large enough to ensure convergence of the results. Besides these, pure numerical conditions, the prospective basis should include all relevant states for the physical process in question. As the incoming Li ion captures the electron mainly in $n = 2, 3, 4$ states the basis we adopted includes all $n \leq 7$ states around Li^{3+} center (84 in total) and all $n \leq 4$ states around the proton center (20 in total). No pseudo states, bound or continuum, are present in the non-screened (pure Coulomb) case $\mathrm{D} \to \infty$. For finite screening parameter D however, some of these bound states enter the continuum and model the coupling with it, more pronounced as the states approach the continuum with decreasing D.

For convergence check we performed computations, for pure Coulomb interaction, with several different bases, changing, systematically the maximum n_{max} for both centers; n_{max} being 6,7 or 8 for Li^{3+} center and 4 or 5 for proton center (see Table 1). The results of these calculations, for three different energies of the impact particle, show that the relative difference of the total electron capture cross section for the adopted basis "$7-4$" (*i.e.* the basis with all $n \leq 7$ on Li^{3+} and all $n \leq 4$ on p) and that for other bases is less than 0.6% for 10.97 keV/u and less than 5%

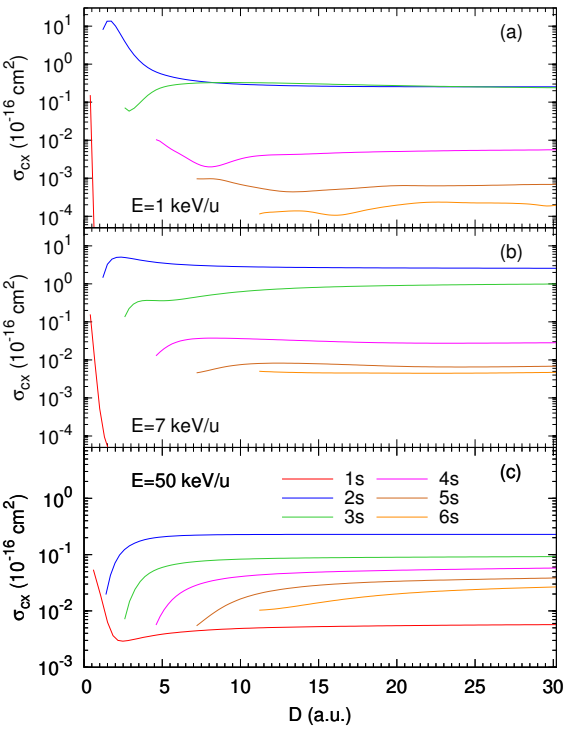

Fig. 2 – (Color online) Electron capture (CX) cross sections for s states ($n \leq 6$), for $D < 30$ a.u., for three different energies: $E = 1$ keV/u (panel (a)), $E = 7$ keV/u (panel (b)) and $E = 50$ keV/u (panel (c)). Note that curves end on their left sides at corresponding critical lengths for the level in question; for lower D the states enter the continuum and CX sections should be properly named as capture-in-continuum (CC) sections. Note the local maxima for $2s$ level around $D \sim 2$ a.u. for $E = 1$ keV/u (panel (a)) and for $E = 7$ keV/u (panel (b)); see the text.

for 107.45 keV/u. We consider this level of convergence as appropriate for the intent of this work. The corresponding relative difference of the sections for 1.0 keV/u approach 10% and together with the failure of the code to deliver numerically stable results with the available hardware, for the two largest bases, limits the validity of our results to energies larger than 1.0 keV/u .

We used the same basis for finite values of screening parameter D. We performed convergence checks for selected D with similar or better relative differences of the total electron capture sections, which gave us confidence to proceed with calculations within entire range of D from 0.5 a.u. to 30 a.u..

As for this system, in the non-screened case, there are numerous theoretical and experimental results for electron capture sections, so we decide, as part of check-

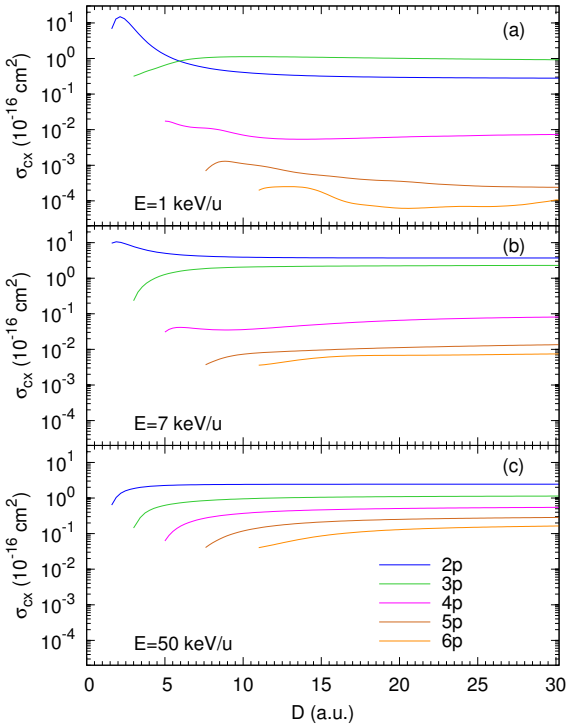

Fig. 3 – (Color online) Same as in Fig. 2 but for p states.

Table 1

Total electron capture sections for several different bases and energies in the non-screened case, calculated as part of convergence check. The basis adopted here contains all single electron $n \leq 7$ states around Li^{3+} center and all $n \leq 4$ electron states around proton center (we refer to this basis as "$7-4$"). For the two largest bases and $E = 1$ keV/u the calculations failed to produce correct result, due to hardware limitations. For details see the text.

basis	1.0 keV/u	10.97 keV/u	107.45 keV/u
$6-4$	0.26611E+01	0.18058E+02	0.14062E+01
$6-5$	0.29319E+01	0.18081E+02	0.14023E+01
$7-4$	0.26713E+01	0.18159E+02	0.14695E+01
$7-5$	0.29517E+01	0.18179E+02	0.14655E+01
$8-4$	-	0.18248E+02	0.14998E+01
$8-5$	-	0.18265E+02	0.14955E+01

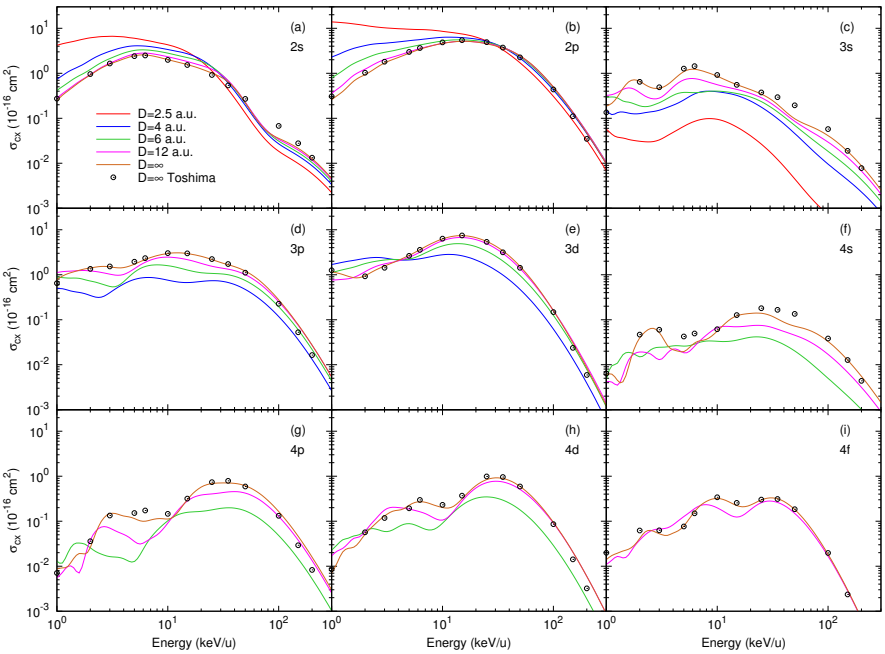

Fig. 4 – (Color online) Energy dependance of state-selective electron capture to nl states ($n \leq 4$) for selected values of screening parameter D as well as for non-screened case, compared with theoretical results of Toshima.

ing the validity of our AOCC calculations, to compare only with the most accurate AOCC results of Toshima and Tawara [11]. The method works quite well in the considered energy range; the slight deviation between our results and those of [11] for medium and higher energies are due to the smaller discrete basis for Li^{3+}, used in [11] consisting of only those states with $n \leq 5$.

3. RESULTS AND DISCUSSION

The Debye-Hückel potential lifts the Coulomb degeneracy for different l and supports a finite number of bound states for any final value of the screening parameter D [12]. With decreasing D the levels enter the continuum at some critical values D^c_{nl} (Table 2), different for Li^{2+} and H (Fig. 1).

For analyzing the dynamics of capturing process two points are highly relevant. Firstly, decreasing the screening length decreases the number of bound states available for capturing. Secondly, the same change decreases the energy difference between the ground state of hydrogen and nl levels of Li^{2+}, and for some states/values

Table 2

Critical screening lengths $D^c_{nl}(a_0)$ for Li^{2+} ($n \leq 6$) ion in the Debye-Hückel potential (upper part) and the corresponding values for H ($n \leq 4$) [10] (lower part).

Li^{2+}						
$n \rightarrow$	1	2	3	4	5	6
$l = 0$	0.275	1.068	2.480	4.458	7.188	11.017
$l = 1$		1.541	2.963	4.931	7.544	11.048
$l = 2$			3.622	5.719	8.385	11.633
$l = 3$				6.655	9.437	12.694
$l = 4$					10.642	14.030
$l = 5$						15.488
H						
$n \rightarrow$	1	2	3	4		
$l = 0$	0.848	3.289	7.353	13.266		
$l = 1$		4.548	8.924	14.947		
$l = 2$			10.951	17.241		
$l = 3$				19.920		

of D it reduces this difference to zero, *i.e.* it makes the aforementioned states energy resonant (see *e.g.* the intersections between $1s$ curve for H and $2l$ curves for Li^{2+} in Fig. 1). Due to these resonances the dependence of the partial cross sections, for the states involved, on the screening length shows a bell-shaped maxima at low energies, see panels (a) on Figs. 2 and 3, for $2s$ and $2p$ states respectively. Both curves show local maxima for $E = 1\,\mathrm{keV/u}$ around $D \sim 2.5\ a.u.$. The same feature is present on panels (b), for $E = 7\,\mathrm{keV/u}$ albeit less pronounced.

The screened potential changes the bound state wave functions too, compared to the pure Coulomb potential. With decreasing D the amplitude in the asymptotic region increases (at small radial distances correspondingly decreases) and so increases the overlap with the initial state [13, 14]. As the electron capture at low collision energies mainly occurs at large internuclear distances, this increased overlap increases the low-energy electron capture cross sections and, for some states, these can be larger than those in the plasma-free case. (Compare the "inversion" of the state-selective electron capture sections to $2l$ states in the low-energy region, below $E \sim 25\,\mathrm{keV/u}$ with respect to other presented nl states on Fig. 4). This phenomenon may be seen present in the energy dependence of the total electron capture sections up to $E \sim 8\,\mathrm{keV/u}$ too (Fig. 6).

A similar behavior of partial cross-sections was noticed for other collisional systems, involving, *e.g.* O^{8+} [14] and C^{6+} [15], in effect down to $Z = 2$ [13] for collision energies below $25\ \mathrm{keV/u}$.

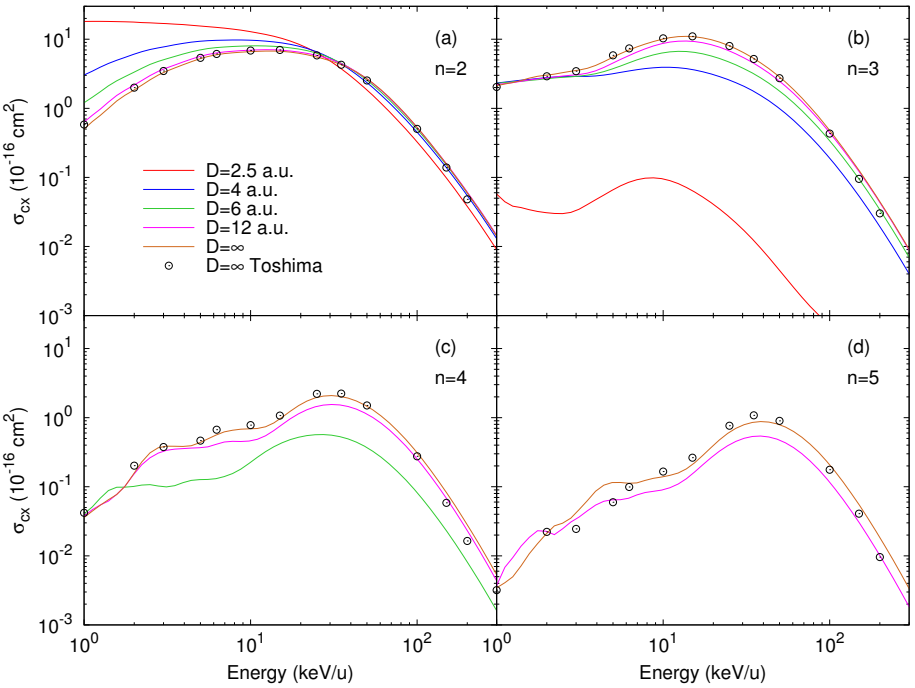

Fig. 5 – (Color online) Energy dependance of electron capture to $n = 2$ states (panel (a)), $n = 3$ states (panel (b)), $n = 4$ states (panel (c)) and to $n = 5$ states (panel (d)) for selected values of screening parameter D and in non-screened case, compared with theoretical results of Toshima. Note that the basis used in [11] includes all $n \leq 5$ states on Li^{3+} only; hence one may expect some deviations from our results for $n = 5$ (panel (d)).

For collisional energies above $E \sim 10$ keV/u the energy dependence of total electron capture sections decreases with decreasing value of the screening length (see Fig. 6) due to predominance of capturing of the electron at smaller internuclear distances where the overlap of the initial and final states gets progressively smaller (for partial sections most clearly visible for $2s$ and $3d$ states - panels (a) and (e) on Fig. 4). On Fig. 2 (panel (c)), for $E = 50$ keV/u one may see the curving down of the lines for partial ns sections with decreasing D; the number of bound levels reduces and as they approach the continuum, with further decreasing of D, the probability for electron capture increases for the deepest, $1s$ state only.

For various values of collisional energy and screening length, which makes unavailable some channels, the multi-state close-coupling description of the electron capture should include the inter-channel couplings and make the physical picture quite complex. One may see the crude traces of this complexity in various minor

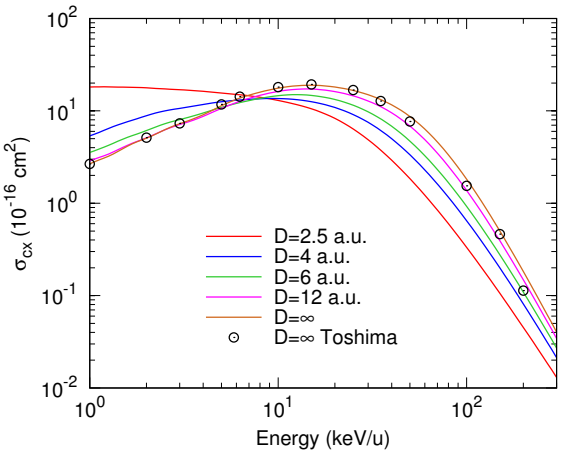

Fig. 6 – (Color online) Energy dependence of total electron capture sections for selected values of screening parameter D and in pure Coulomb case interaction, compared with theoretical results of Toshima.

structures in the partial sections, for the dominantly populated $n = 2$ to $n = 4$ levels. We note that for the highest level some structures may be computational artifacts and of nonphysical origin.

4. CONCLUSIONS

The screening interaction between two charged centers and the electron lifts the $l-$ degeneracy of the Coulomb potential, changes the number of bound states and their wave-functions, decreases their amplitudes for smaller distances, and increases them in the asymptotic region. For the collisional system $\mathrm{Li}^{3+} + \mathrm{H}(1s)$ it means that the $2l$ levels of $\mathrm{Li}^{2+}(nl)$ system are getting energy resonant with the ground state of hydrogen atom in parametric region around $\mathrm{D} \sim 2$ a.u.. Therefore, the partial sections for electron capture into $2l$ states get enhanced for low-energy collisions for which the transfer of the electron occurs at large distances, with decreasing D due to two factors: firstly, increase of the corresponding matrix element due to increase overlap of the initial and final states in the asymptotic region, and, secondly, decrease of the energy defect of the involved levels which, for some D are energy resonant. For higher energies, the region of capturing shifts to smaller distances and the partial sections reduce due to reduced amplitudes there, of the radial wave functions of the electron in the states involved.

The magnitude and the energy behavior of the electron capture sections in the intermediate region of energies are shaped by the relative dominance of these two factors. The smaller, local structures, visible in these sections, result from multi-state

couplings. For a more complete explanation of these structures within the AOCC framework one has to use larger bases. In the low-energy region one may employ the MOCC method too but, to the best of our knowledge, such studies have not been published so far.

REFERENCES

1. D. Salzman, *Atomic Physics in Hot Plasma*, Oxford University Press, Oxford, 1998.
2. R. K. Janev and H. Winter, Phys. Rep. **117**, 265 (1985).
3. W. Fritsch and C. D. Lin, Phys. Rep. **202**, 1 (1991).
4. A. Loarte *et al.*, Nucl. Fusion **47**, S203 (2007).
5. F. Aumayr *et al.*, J. Nucl. Mater. **196-198**, 928 (1992).
6. L. L. Yan *et al.*, Eur. Phys. J. D **69**, 26 (2015).
7. B. H. Bransden and M. R. R. McDowell, *Charge Exchange and the Theory of Ion-Atom Collisions*, Clarendon Press, Oxford, 1992.
8. J. Kuang and C. D. Lin, J. Phys. B **30**, 101 (1997).
9. C. M. Reeves, J. Chem. Phys. **39**, 1 (1963).
10. F. J. Rogers, H. C. Graboske, and D. J. Harwood, Phys. Rev. A **1**, 1577 (1970).
11. N. Toshima and H. Tawara, *Excitation, Ionization, and Electron Capture Cross Sections of Atomic Hydrogen in Collision with Multiply Charge Ions*, NIFS-DATA **26**, July 1995.
12. L. D. Landau and E. M. Lifshitz, *Quantum Mechanics: Non-Relativistic Theory*, Pergamon, London, 1958.
13. L. Liu, J. G. Wang, and R. K. Janev, Phys. Rev A **77**, 032709 (2008).
14. L. Liu, J. G. Wang, and R. K. Janev, Phys. Rev. A **79**, 052702 (2009).
15. D. Jakimovski, L. Liu, J. G. Wang, and R. K. Janev, J. Phys. B: At. Mol. Opt. Phys. **43**, 165202 (2010).